EARTH HISTORY

The Anthropocene is functionally and stratigraphically distinct from the Holocene

Colin N. Waters,* Jan Zalasiewicz, Colin Summerhayes, Anthony D. Barnosky, Clément Poirier, Agnieszka Gałuszka, Alejandro Cearreta, Matt Edgeworth, Erle C. Ellis, Michael Ellis, Catherine Jeandel, Reinhold Leinfelder, J. R. McNeill, Daniel deB. Richter, Will Steffen, James Syvitski, Davor Vidas, Michael Wagreich, Mark Williams, An Zhisheng, Jacques Grinevald, Eric Odada, Naomi Oreskes, Alexander P. Wolfe

BACKGROUND: Humans are altering the planet, including long-term global geologic processes, at an increasing rate. Any formal recognition of an Anthropocene epoch in the geological time scale hinges on whether humans have changed the Earth system sufficiently to produce a stratigraphic signature in sediments and ice that is distinct from that of the Holocene epoch. Proposals for marking the start of the Anthropocene include an "early Anthropocene" beginning with the spread of agriculture and deforestation; the Columbian Exchange of Old World and New World species; the Industrial Revolution at ~1800 CE; and the mid-20th century "Great Acceleration" of population growth and industrialization.

ADVANCES: Recent anthropogenic deposits contain new minerals and rock types, reflecting rapid global dissemination of novel materials including elemental aluminum, concrete, and plastics that form abundant, rapidly evolving "technofossils." Fossil fuel combustion has disseminated black carbon, inorganic ash spheres, and spherical carbonaceous particles worldwide, with a near-synchronous global increase around 1950. Anthropogenic sedimentary fluxes have intensified, including enhanced erosion caused by deforestation and road construction. Widespread sediment retention behind dams has amplified delta subsidence.

Geochemical signatures include elevated levels of polyaromatic hydrocarbons, polychlorinated biphenyls, and pesticide residues, as well as increased $^{207/206}$Pb ratios from leaded gasoline, starting between ~1945 and 1950. Soil nitrogen and phosphorus inventories have doubled in the past century because of increased fertilizer use, generating widespread signatures in lake strata and nitrate levels in Greenland ice that are higher than at any time during the previous 100,000 years.
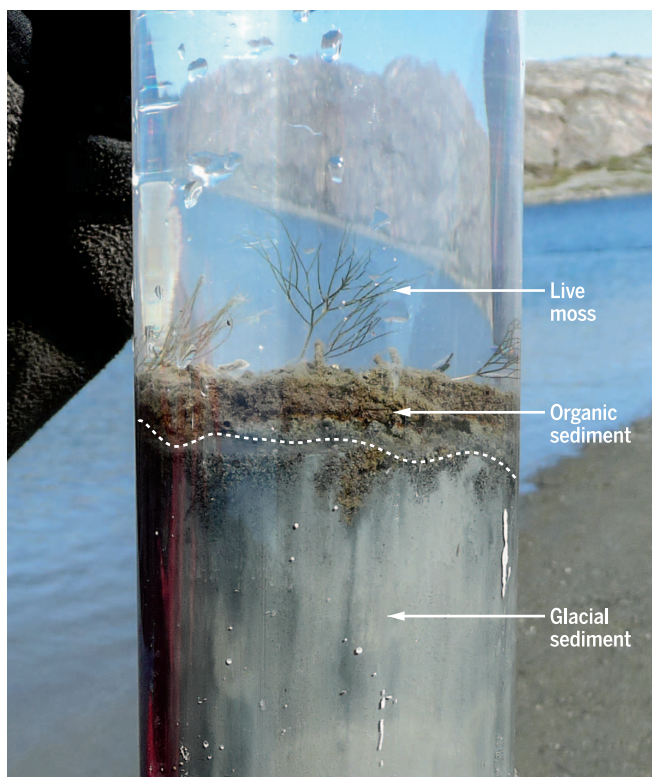
Indicators of the Anthropocene in recent lake sediments differ markedly from Holocene signatures. These include unprecedented combinations of plastics, fly ash, radionuclides, metals, pesticides, reactive nitrogen, and consequences of increasing greenhouse gas concentrations. In this sediment core from west Greenland (69°03'N, 49°54'W), glacier retreat due to climate warming has resulted in an abrupt stratigraphic transition from proglacial sediments to nonglacial organic matter, effectively demarcating the onset of the Anthropocene. [Photo credit: J. P. Briner]

Detonation of the Trinity atomic device at Alamogordo, New Mexico, on 16 July 1945 initiated local nuclear fallout from 1945 to 1951, whereas thermonuclear weapons tests generated a clear global signal from 1952 to 1980, the so-called "bomb spike" of excess ^{14}C, ^{239}Pu, and other artificial radionuclides that peaks in 1964.

Atmospheric CO_2 and CH_4 concentrations depart from Holocene and even Quaternary patterns starting at ~1850, and more markedly at ~1950, with an associated steep fall in δ^{13}C

that is captured by tree rings and calcareous fossils. An average global temperature increase of 0.6° to 0.9°C from 1900 to the present, occurring predominantly in the past 50 years, is now rising beyond the Holocene variation of the past 14,000 years, accompanied by a modest enrichment of δ^{18}O in Greenland ice starting at ~1900. Global sea levels increased at 3.2 ± 0.4 mm/year from 1993 to 2010 and are now rising above Late Holocene rates. Depending on the trajectory of future anthropogenic forcing, these trends may reach or exceed the envelope of Quaternary interglacial conditions.

Biologic changes also have been pronounced. Extinction rates have been far above background rates since 1500 and increased further in the 19th century and later; in addition, species assemblages have been altered worldwide by geologically unprecedented transglobal species invasions and changes associated with farming and fishing, permanently reconfiguring Earth's biological trajectory.

OUTLOOK: These novel stratigraphic signatures support the formalization of the Anthropocene at the epoch level, with a lower boundary (still to be formally identified) suitably placed in the mid-20th century. Formalization is a complex question because, unlike with prior subdivisions of geological time, the potential utility of a formal Anthropocene reaches well beyond the geological community. It also expresses the extent to which humanity is driving rapid and widespread changes to the Earth system that will variously persist and potentially intensify into the future. ∎

EARTH HISTORY

The Anthropocene is functionally and stratigraphically distinct from the Holocene

Colin N. Waters,[1]* Jan Zalasiewicz,[2] Colin Summerhayes,[3] Anthony D. Barnosky,[4] Clément Poirier,[5] Agnieszka Gałuszka,[6] Alejandro Cearreta,[7] Matt Edgeworth,[8] Erle C. Ellis,[9] Michael Ellis,[1] Catherine Jeandel,[10] Reinhold Leinfelder,[11] J. R. McNeill,[12] Daniel deB. Richter,[13] Will Steffen,[14] James Syvitski,[15] Davor Vidas,[16] Michael Wagreich,[17] Mark Williams,[2] An Zhisheng,[18] Jacques Grinevald,[19] Eric Odada,[20] Naomi Oreskes,[21] Alexander P. Wolfe[22]

Human activity is leaving a pervasive and persistent signature on Earth. Vigorous debate continues about whether this warrants recognition as a new geologic time unit known as the Anthropocene. We review anthropogenic markers of functional changes in the Earth system through the stratigraphic record. The appearance of manufactured materials in sediments, including aluminum, plastics, and concrete, coincides with global spikes in fallout radionuclides and particulates from fossil fuel combustion. Carbon, nitrogen, and phosphorus cycles have been substantially modified over the past century. Rates of sea-level rise and the extent of human perturbation of the climate system exceed Late Holocene changes. Biotic changes include species invasions worldwide and accelerating rates of extinction. These combined signals render the Anthropocene stratigraphically distinct from the Holocene and earlier epochs.

The term "Anthropocene" is currently used informally to encompass different geological, ecological, sociological, and anthropological changes in recent Earth history. The origins of the concept of the Anthropocene, its terminology, and its sociopolitical implications are widely discussed (*1, 2*). When considering the stratigraphic definition of the Anthropocene, there are two basic questions: Have humans changed the Earth system to such an extent that recent and currently forming geological deposits include a signature that is distinct from those of the Holocene and earlier epochs, which will remain in the geological record? If so, when did this stratigraphic signal (not necessarily the first detectable anthropogenic change) become recognizable worldwide? These questions are considered here in the context of how stratigraphic units have been formally recognized earlier in the Quaternary period.

Proposals for marking the start of the Anthropocene have included (i) an "early Anthropocene" associated with the advent of agriculture, animal domestication, extensive deforestation, and gradual increases in atmospheric carbon dioxide (CO_2) and methane (CH_4) levels thousands of years ago (*3, 4*); (ii) the Columbian Exchange of Old World and New World species associated with colonization of the Americas (*5*); (iii) the beginning of the Industrial Revolution at ~1800 CE (*6, 7*); and (iv) the mid-20th century "Great Acceleration" of population growth, industrialization, and mineral and energy use (*8–10*).

Here we review several lines of evidence suggesting that the Anthropocene's stratigraphic signatures distinguish it from the Holocene (Fig. 1). We find that criteria available to recognize the Anthropocene are consistent with those used to define other Quaternary stratigraphic units. Earlier Quaternary time-unit subdivisions are defined by signals from cyclical forcings of climate change, such as variation in Earth's orbit or solar irradiance, and irregular events such as volcanic eruptions. Although these forcings continue, the Anthropocene markers reflect an additional key driver, that of human modification of global environments at unprecedented rates. This driver has produced a wide range of anthropogenic stratigraphic signals (Fig. 1), including examples that are novel in Earth history, that are global in extent, and that offer fine temporal resolution. The signals vary in their development: Some are already advanced, and others are at early stages. We describe these signals and suggest how they may be used in the stratigraphic characterization and correlation of a formalized Anthropocene epoch with a lower boundary (still to be identified) potentially placed in the mid-20th century.

How are Quaternary stratigraphic units defined?

The Quaternary period, which began 2.6 million years ago (Ma), is subdivided into geochronological time units (epochs and ages) with boundaries that are linked at least in part to climate change events (expressed as marine isotope stages), in association with paleomagnetic reversals (*11*). This contrasts with the subdivision of most of the Phanerozoic eon (the past ~541 ± 1 Ma), for which the first or last appearance of key fossil taxa is typically used to define time units. Fossil-based boundaries represent change at rates too slow and time-transgressive for the geologically recent past, in which the time units are of comparatively short duration (about 12,000 years for the Holocene versus 2 million years or more for earlier epochs). These time intervals are recognizable in the geologic record as chronostratigraphic units (series and stages), which, in contrast to the time units, are physical entities, including rocks, sediments, and glacier ice. Ideally, a chronostratigraphic unit is exemplified, and its lower boundary defined, at a single locality termed the Global Boundary Stratotype Section and Point (GSSP), which is typically in marine strata for pre-Holocene series (*12*).

The start of the Holocene epoch (or series) is based on the termination of the transition from the last glacial phase into an interval of warming accompanied by ~120 m of sea-level rise. The warming took place over about 1600 years and is recorded by a variety of stratigraphic signals that are not all globally synchronous. In the Northern Hemisphere, the signal for the Holocene's beginning

[1]British Geological Survey, Keyworth, Nottingham NG12 5GG, UK. [2]Department of Geology, University of Leicester, University Road, Leicester LE1 7RH, UK. [3]Scott Polar Research Institute, Cambridge University, Lensfield Road, Cambridge CB2 1ER, UK. [4]Department of Integrative Biology, Museum of Paleontology, and Museum of Vertebrate Zoology, University of California–Berkeley, Berkeley, CA 94720, USA. [5]Morphodynamique Continentale et Côtière, Université de Caen Normandie, Centre National de la Recherche Scientifique (CNRS), 24 Rue des Tilleuls, F-14000 Caen, France. [6]Geochemistry and the Environment Division, Institute of Chemistry, Jan Kochanowski University, 15G Świętokrzyska Street, 25-406 Kielce, Poland. [7]Departamento de Estratigrafía y Paleontología, Facultad de Ciencia y Tecnología, Universidad del País Vasco/Euskal Herriko Unibertsitatea, Apartado 644, 48080 Bilbao, Spain. [8]School of Archaeology and Ancient History, University of Leicester, University Road, Leicester LE1 7RH, UK. [9]Department of Geography and Environmental Systems, University of Maryland–Baltimore County, Baltimore, MD 21250, USA. [10]Laboratoire d'Etudes en Géophysique et Océanographie Spatiales (CNRS, Centre National d'Études Spatiales, Institut de Recherche pour le Développement, Université Paul Sabatier), 14 Avenue Edouard Belin, 31400 Toulouse, France. [11]Department of Geological Sciences, Freie Universität Berlin, Malteserstraße 74-100/D, 12249 Berlin, Germany. [12]Georgetown University, Washington, DC, USA. [13]Nicholas School of the Environment, Duke University, Box 90233, Durham, NC 27516, USA. [14]The Australian National University, Canberra, Australian Capital Territory 0200, Australia. [15]Department of Geological Sciences, University of Colorado–Boulder, Box 545, Boulder, CO 80309-0545, USA. [16]Marine Affairs and Law of the Sea Programme, The Fridtjof Nansen Institute, Lysaker, Norway. [17]Department of Geodynamics and Sedimentology, University of Vienna, A-1090 Vienna, Austria. [18]State Key Laboratory of Loess and Quaternary Geology, Institute of Earth Environment, Chinese Academy of Sciences, Xi'an 710061, Beijing Normal University, Beijing 100875, China. [19]Institut de Hautes Études Internationales et du Développement, Chemin Eugène Rigot 2, 1211 Genève 11, Switzerland. [20]Department of Geology, University of Nairobi, Nairobi, Kenya. [21]Department of History of Science, Harvard University, Cambridge, MA 02138, USA. [22]Department of Biological Sciences, University of Alberta, Edmonton, Alberta T6G 2E9, Canada.
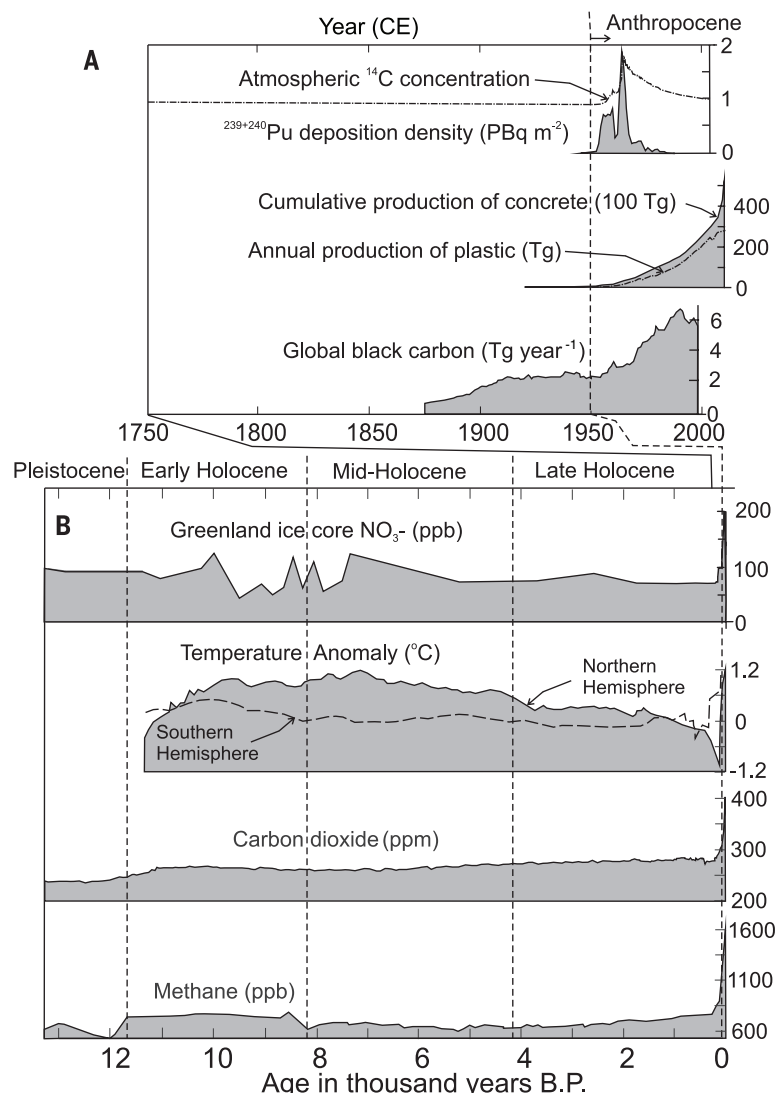*Corresponding author. E-mail: cnw@bgs.ac.uk

Fig. 1. Summary of the magnitude of key markers of anthropogenic change that are indicative of the Anthropocene. (**A**) Novel markers, such as concrete, plastics, global black carbon, and plutonium (Pu) fallout, shown with radiocarbon (^{14}C) concentration. (**B**) Long-ranging signals such as nitrates (NO_3^-), CO_2, CH_4, and global temperatures, which remain at relatively low values before 1950, rapidly rise during the mid-20th century and, by the late 20th century, exceed Holocene ranges.

was taken as the abrupt end of the Younger Dryas cooling event. The GSSP chosen to define the base of the Holocene was agreed to lie within the NGRIP2 ice core from central Greenland (NGRIP, North Greenland Ice Core Project) (*13*). The core contains a detailed archive of environmental change, preserved in the composition of air bubbles trapped in the ice and in the chemical and physical characteristics of the ice. The GSSP lies within a multidecade warming and moistening trend, which is inferred from oxygen isotopes showing rising δ^{18}O, associated with a reduction in dust content. About midway through this trend, the sharpest change is a decrease in excess deuterium, which is interpreted as representing a re-organization of North Atlantic ocean-atmosphere circulation at 11,700 years before the year 2000 CE, ± 99 years at 2σ (*13*). This distinctive change is used to define the base of the Holocene series (the material chronostratigraphic unit). Thus,

by definition, the Holocene epoch (the abstract time unit) began ~11,700 years ago.

The Holocene epoch (and corresponding series) is being considered for subdivision into three component sub-epochs (subseries), again using climatic signatures to guide the positioning of their bases. The base of the Lower Holocene, by default, would be the base of the Holocene series, as described above. The base of the Middle Holocene has been proposed to lie within a short-lived (150 ± 30 years) cooling event at 8200 years before the present (yr B.P.), where there is a marked shift to lower ^{18}O/^{16}O values (more negative δ^{18}O values) within the NGRIP1 ice core in the Greenland Ice Sheet (*13*). Within the same narrow interval of time, Greenland ice cores show low deuterium/hydrogen (D/H) ratios, a decline in annual layer thickness, an atmospheric CH_4 minimum, and a volcanic marker characterized by high fluoride content. Such signals have led

to the proposal that a Greenland ice core should be used to define the Middle Holocene GSSP (*13*). Although such signals are most strongly evident at localities adjacent to the North Atlantic, they probably make up part of a global signature, because correlative signals are evident in lake sediments as changes in pollen assemblages and oxygen isotopes; in cave speleothems as isotopic signals reflecting changes in the intensity of the South American monsoon; in marine foraminiferal assemblages (species compositions); and in increased aridification around the Mediterranean that broadly coincides with the Mesolithic-Neolithic transition (*13*).

The base of the Upper Holocene has been proposed to lie at a mid- and low-latitude aridification event at 4200 yr B.P. (*13*). This event appears to have coincided with cooling of the North Atlantic and tropical Pacific, the arrival of cooler and wetter conditions in Europe, and a weakening of the Asian monsoon (*13*). The proposed stratotype is in a speleothem record from Mawmluh Cave in northeast India, at the midpoint of a two-stage shift of δ^{18}O values in calcite from more positive, starting at 4300 yr B.P., to more negative, starting at 4100 yr B.P. (*13*). Although there is no doubt that marked environmental perturbations occurred at both 8200 and 4200 yr B.P., most proxies indicate subsequent recovery in a matter of centuries, implying that these were temporally discrete paleoclimatic events as opposed to truly novel states within the Earth system.

Human drivers of stratigraphic signatures

The driving human forces responsible for many of the anthropogenic signatures are a product of the three linked force multipliers: accelerated technological development, rapid growth of the human population, and increased consumption of resources. These have combined to result in increased use of metals and minerals, fossil fuels, and agricultural fertilizers and increased transformation of land and nearshore marine ecosystems for human use. The net effect has been a loss of natural biomes to agriculture, cities, roads, and other human constructs and the replacement of wild animals and plants by domesticated species to meet growing demands for food. This increase in consumption of natural resources is closely linked to the growth of the human population. Anatomically modern *Homo sapiens* emerged ~200,000 years ago (*14*). By 12,000 yr B.P., around the start of the Holocene, humans had colonized all of the continents except Antarctica and the South Pacific islands and had reached a total population estimated at 2 million (*15*, *16*). Up to this point, human influence on the Earth system was small relative to what has happened since the mid-20th century; even so, human impacts contributed to the extinction of Pleistocene megafauna (*17*). However, the key signals used to recognize the start of the Holocene epoch were not directly influenced by human forcing, which is a major distinction from the proposed Anthropocene epoch.

Humans had a growing stratigraphic influence throughout the Holocene epoch as the global population gradually increased. It has been argued that ~8000 years ago, with a global population estimated at less than 18 million ([15], [16]), the initiation of agricultural practices and forest clearances began to gradually increase atmospheric CO_2 levels ([3]). But it was not until ~1800 CE that the global population first reached 1 billion ([16]). Increased mechanization and the drive to urbanization during the Industrial Revolution, initially in Western Europe and eventually worldwide ([18]), then facilitated a more rapid population increase. Although this population growth is commonly thought to have increased exponentially through the 19th and 20th centuries ([8], [9]), recent analyses ([15], [16]) suggest that it can be differentiated into a period of relatively slower growth from 1750 to 1940 CE and one of more rapid growth from 1950 to 2010 CE. The inflection point at ~1950 CE coincides with the Great Acceleration ([8], [9]), a prominent rise in economic activity and resource consumption that accounts for the marked mid-20th century upturns in or inceptions of the anthropogenic signals detailed below.

New anthropogenic materials

Recent anthropogenic deposits, which are the products of mining, waste disposal (landfill), construction, and urbanization ([19]), contain the greatest expansion of new minerals since the Great Oxygenation Event at 2400 Ma ([20]) and are accompanied by many new forms of "rock," in the broad sense of geological materials with the potential for long-term persistence. Over many millennia, humans have manufactured materials previously unknown on Earth, such as pottery, glass, bricks, and copper alloys. Remains of these materials are present as a persistent and widespread geological signal that is markedly time-transgressive, reflecting the migration of peoples ([21]). In contrast, elemental aluminum, which was almost unknown in native form before the 19th century, has seen 98% of its cumulative global production of ~500 Tg since 1950 CE (Fig. 2A) ([20], [22]). Concrete, which was invented by the Romans, became the primary building material from World War II (1939–1945 CE) onward. The past 20 years (1995–2015) account for more than half of the 50,000 Tg of concrete ever produced ([22], [23]) (Fig. 2A), equivalent to ~1 kg m^{-2} of the planet surface. Concrete and aluminum are widely disseminated across terrestrial, particularly urban, settings.

Similarly, the manufacture of new organic polymers (plastics), which were initially developed in the early 1900s, rapidly grew from the 1950s to an annual production of about ~300 Tg in 2013 ([24]) (Fig. 2A), comparable to the present human biomass. Plastics spread rapidly via rivers into lakes, and they are now also widespread in both shallow- and deep-water marine sediments as macroscopic fragments and as virtually ubiquitous microplastic particles (microbeads, "nurdles," and fibers) (Fig. 2A) ([25]–[27]), which are dispersed by both physical and biological processes. The decay resistance and chemistry of most plastics
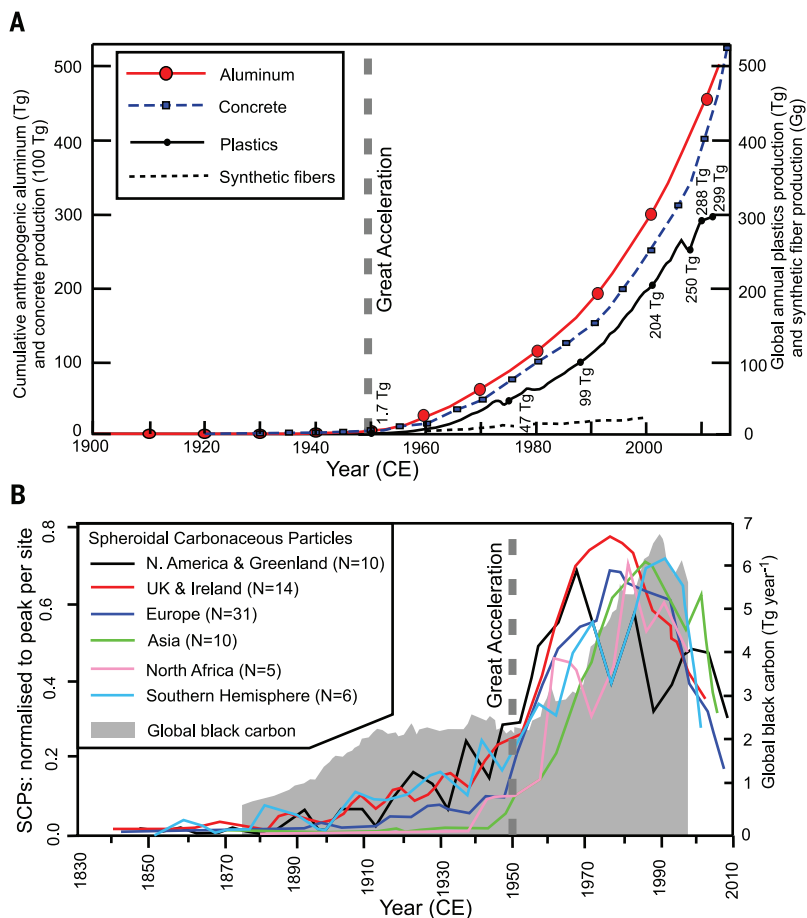

Fig. 2. The production of selected new anthropogenic materials. (**A**) Cumulative growth of manufactured aluminum in the surface environment [adapted from data in ([23]), assuming a recycling rate of 50%]; cumulative growth of production of concrete, assuming that most cement goes into concrete and that ~15% of average concrete mass is cement [from ([22]), derived from U.S. Geological Survey global cement production statistics]; annual growth of plastics production [from ([24])]; and synthetic fibers production [from ([26])]. (**B**) Global mid–20th century rise and late–20th century spike in SPCs, normalized to the peak value in each lake core [modified from ([32])], and global black carbon from available annual fossil fuel consumption data for 1875–1999 CE ([30]). Numbers of lake cores for each region are indicated.

suggest that they will leave identifiable fossil and geochemical records.

These and other new materials are commonly shaped into abundant artifacts with the capacity to be preserved in and to help date future geological deposits. Analogous to biotic fossil remains, these so-called technofossils ([28]) provide annual to decadal stratigraphic resolution ([19], [22])—far greater than what can be obtained from the first and last appearances of fossil taxa, which have traditionally been the most common means of correlating stratal sections ([29]).

Fossil fuel combustion disseminates unburned particles as black carbon, inorganic ash spheres (IASs), and spherical carbonaceous particles (SCPs). Black carbon increased markedly toward the end of the 19th century, and especially after ~1970 CE, with a peak at 6.7 Tg year^{-1} in ~1990 CE (Fig. 2B) ([30]). IASs, which are locally detectable in the stratigraphic record starting in the 16th century, increased across Britain, Scandinavia, and North America from ~1835 to 1960 CE ([31]). SCPs, which

were first recorded at various sites in the UK from 1830 to 1860 CE, show a near-synchronous global increase around 1950 CE, with peak signatures from the 1960s to the 1990s (Fig. 2B) ([32], [33]). Black carbon, IASs, and SCPs, being airborne particulates, leave a permanent marker within both sediments and glacial ice. An ancient analog is the marker horizon of carbon impact spherules at the Cretaceous-Paleogene boundary, which was created by the Chicxulub bolide impact ([34]). These low-temperature natural spherules, which are readily distinguishable from high-temperature industrial SCPs, demonstrate the likely persistence of SCPs as a stratigraphic marker ([32]).

Modification of sedimentary processes

The transformation of more than 50% of Earth's land surface for human use ([35]) has generated anthropogenically modified materials that extend across multiple terrestrial settings. They are most ubiquitous in anthropogenic (artificial) deposits such as landfills, urban structures, and mine tailings,
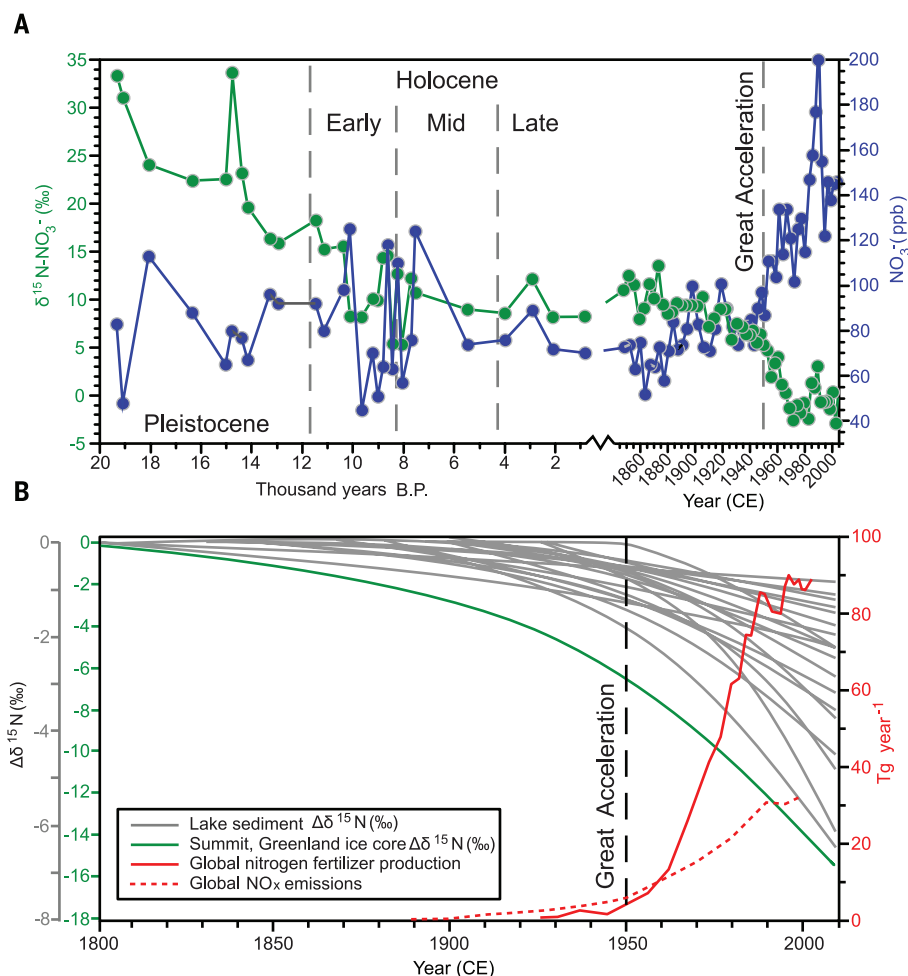
A

B

Fig. 3. Perturbations of the nitrogen cycle since the start of the Late Pleistocene. (**A**) Coevolution of ice core NO$_3^-$ (blue) and δ^{15}N for NO$_3^-$ (green) from the Late Pleistocene to the present, obtained by splicing data from two cores from Summit, Greenland (72.5°N, 38.4°W, 3200 m above sea level) (55–57). (**B**) Power functions fitted to δ^{15}N data from lake sediments (gray lines, representing 25 remote Northern Hemisphere sites) and ice cores (green line), expressed as departures (Δδ^{15}N) from preindustrial baseline values (53, 54). These isotopic trends are shown alongside annual rates of reactive N production from agricultural fertilizer (solid red line) and NO$_x$ emissions from fossil fuel combustion (dashed red line) (51).

built in the past 60 years, at an average rate of more than one large dam per day (8, 9), and each will last 50 to 200 years, interrupting sediment transport to the oceans. The reduced sediment flux to major deltas, combined with increasing extraction of groundwater, hydrocarbons, and sediments (for aggregates), has caused many large deltas to subside more quickly, a process beginning in the 1930s (43) at rates faster than modern eustatic sea-level rise. Coastal retreat is an inevitable result. These various signals, which are abrupt on geological time scales, are diachronous at the decadal scale.

Changed geochemical signatures in recent sediments and ice

Anthropogenic materials and the human influence on sedimentary environments have a near-global expression, but geochemical signatures, particularly those with airborne transport pathways, reach all global environments, including the ~12% of Earth's surface that is permanently covered by ice. Among the many distinct geochemical signatures that human activities have introduced into the sedimentary record are elevated concentrations of polyaromatic hydrocarbons, polychlorinated biphenyls, and diverse pesticide residues, each beginning at ~1945 to 1950 CE (44–47). Lead smelting during Roman times resulted in a distinctive local marker of increased $^{207/206}$Pb ratios, a signal that changed globally in the early 20th century as a result of vehicles powered by leaded gasoline (47). This illustrates that some anthropogenic geochemical signatures may vary geographically in their first appearance but nevertheless become useful as global markers when they rapidly spread as the result of new technologies in the mid-20th century.

Nitrogen (N) and phosphorus (P) in soils have doubled in the past century because of increased fertilizer use (8, 9, 48). Production of P by mining, now at ~23.5 Tg year^{-1}, is twice the background weathering rate of P released during the Holocene (49). Human processes are argued to have had the largest impact on the nitrogen cycle for some 2.5 billion years (48). The use of the Haber-Bosch process from 1913 CE onward has increased the amount of reactive N in the Earth system by 120% relative to the Holocene baseline (50), accompanied by an increased flux of nitrogen oxides (NO$_x$) from the combustion of fossil fuels (Fig. 3) (51).

These changes have stratigraphic consequences. The influx of excess reactive N and P to lakes and seas has led to seasonal oxygen deficiency, affecting local microbiota and, in extreme cases, increasing mortality in macrobiota (52). Northern Hemisphere lakes show increasingly depleted δ^{15}N values (53, 54) beginning at ~1895 CE (Fig. 3B) and accelerating over the past 60 years. In Greenland ice, δ^{15}N values during the Late Pleistocene glaciation show a gradual marked decline to a pre-industrial Holocene norm [mean, 9.7 per mil (‰) in the GISP2 (Greenland Ice Sheet Project 2) ice core; (55)]; they decline again and more rapidly starting at ~1850 CE, with the greatest decline occurring between 1950 and 1980 CE (Fig. 3A) (47, 56). The main phase of the increase in nitrate

in addition to soils associated with cultivation. This influence is increasingly extending into the oceans, both directly, through coastal reclamation works, sediment reworking by trawler fishing, and the extraction of sand and gravel; and indirectly, through changes in coastal sedimentary facies in response to rising sea levels, the eutrophication of coastal environments, and coral bleaching events (36). Human land alteration also increasingly extends into the subsurface via drilling into Earth's crust to extract minerals, to store wastes, or to host utilities (37). Mineral extraction alone accounts for the displacement of ~57,000 Tg year^{-1} of sediments, exceeding the current rate of riverborne sediment transport by almost a factor of 3 (38).

Human activities have also modified sedimentary processes sufficiently to leave clear expressions in river, lake, windblown, and glacial deposits (36). Sediment fluxes in many fluvial systems increased historically because of greater defores-

tation, livestock grazing, and cropland development. Clearing of primary forests for agriculture, usually by burning, began in Early to Mid-Holocene times, especially in temperate woodland biomes; this shifted diverse primary forest communities toward domesticates and early successional species and left widespread, time-transgressive geological traces that include profound shifts in plant and animal remains, charcoal, and sediment deposits from soil erosion (39, 40). In recent decades, secondary forests have recovered across much of the temperate zone, and forest clearing has shifted toward tropical regions; for example, periods of rapid deforestation have occurred in Amazonia, Indonesia, and other regions in Asia and Africa in response to economic and governance dynamics (41). The construction of mountain roads in these tropical regions is resulting in substantial surface erosion and landslides (42).

Extensive sediment retention behind dams constructed across major river systems has created a global signal more rapidly. Most dams were

levels also occurred between 1950 and 1980 CE (Fig. 3, A and B), culminating in values higher than any recorded for the previous 100,000 years (57). These markers are distinct from Holocene and Late Pleistocene background levels.

Industrial metals such as cadmium, chromium, copper, mercury, nickel, lead, and zinc have been widely and rapidly dispersed since the mid-20th century, although many show much earlier and markedly diachronous signals associated with the expansion of mineral extraction and processing (47, 58). An acceleration in the use of trace metals and rare earth elements (REEs) began after World War II, resulting in an increase in the amounts mined, a global pattern of dispersion in the environment, and novel stoichiometric ratios. Metals and their derivatives are spread through inadequate processing, a lack of recycling and reuse, or loss during everyday use. For example, platinum, rhodium, and palladium lost from automotive catalytic converters accumulate preferentially in soils adjacent to highways (59).

Radiogenic signatures and radionuclides in sediments and ice

Potentially the most widespread and globally synchronous anthropogenic signal is the fallout from nuclear weapons testing. The start of the Anthropocene may thus be defined by a Global Standard Stratigraphic Age (GSSA) coinciding with detonation of the Trinity atomic device at Alamogordo, New Mexico, on 16 July 1945 CE (10). However, fallout from 1945 to 1951 CE came from fission devices and resulted in only localized deposition of radionuclides. Aggregate yields from thermonuclear weapon tests that began in 1952 CE and peaked in 1961–1962 CE left a clear and global signature, concentrated in the mid-latitudes and highest in the Northern Hemisphere, where most of the testing occurred (Fig. 4B) (47, 60, 61). Useful potential markers include excess ^{14}C, an isotope common in nature, and ^{239}Pu, a naturally rare isotope. The Holocene segment of the IntCal13 Δ^{14}C curve, corrected for radiogenic decay (F^{14}C), shows past natural fluctuations and a linear normalized decrease from 1.2 to ~1.0 during the Holocene, related to changes in the ^{14}C production rate and global carbon cycling (62) (Fig. 4A). An excess of ^{14}C forms a sharp bomb spike, starting in 1954 (10) and peaking in 1964 CE (5), both of which years have been suggested as potential markers for the start of the Anthropocene. However, the peak is diachronous between hemispheres (Fig. 4B) (63). ^{239}Pu, with its long half-life (24,110 years), low solubility, and high particle reactivity, particularly in marine sediments, may be the most suitable radioisotope for marking the start of the Anthropocene (61, 64). The appearance of a ^{239}Pu fallout signature in 1951 CE, peaking in 1963–1964 CE (Fig. 4B), will be identifiable in sediments and ice for the next 100,000 years (61, 64); it will decay to a layer enriched in ^{235}U and, ultimately, stable ^{207}Pb.

Carbon cycle evidence from ice cores

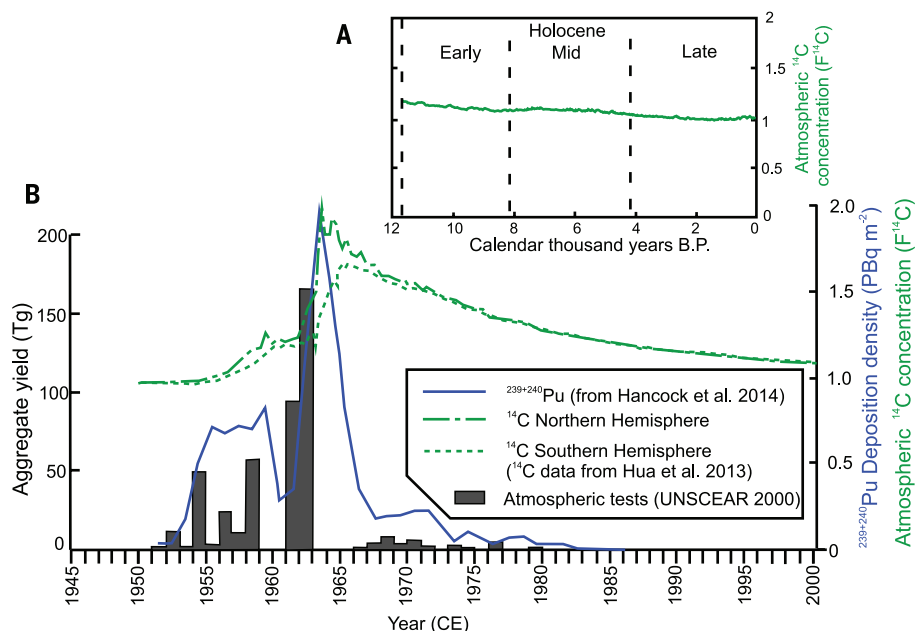Atmospheric CO_2, now above 400 parts per million (ppm), was emitted into the atmosphere

Fig. 4. Radiogenic fallout signals as a marker of the Anthropocene. (A) Age-corrected atmospheric ^{14}C concentration (F^{14}C) based on the IntCal13 curve, before nuclear testing (62). (B) The atmospheric concentration of ^{14}C (F^{14}C) (63) and $^{239+240}$Pu (64) radiogenic fallout from nuclear weapons testing (PBq, petabecquerel), plotted against annual aggregate atmospheric weapons test yields (60).

from 1999 to 2010 CE ~100 times as fast as the most rapid emission during the last glacial termination (65), and concentrations have exceeded Holocene levels since at least 1850 CE (Fig. 5). During the Late Pleistocene to Early Holocene, atmospheric CO_2 preserved in air bubbles in Antarctic glacial ice underwent a stepped 70-ppm rise over 6000 years (66, 67), or an average rise of 1 ppm per ~85 years. Subsequent Holocene CO_2 concentrations remained approximately stable (Fig. 5A). CO_2 concentrations showed a slightly decreasing trend from ~11,000 to 8000 yr B.P. This changed to a slightly rising trend, with a very slow rise of 260 to 285 ppm from ~7000 yr B.P. to the start of the Industrial Revolution (Fig. 5A), a change which has been ascribed to early human agriculture by some (3), albeit controversially (66). Thus, the putative anthropogenic impact on atmospheric CO_2 at this time was both gradual and much less than subsequent changes over the past 200 years. The events at 8200 and 4200 yr B.P. that mark the proposed Mid- and Late Holocene sub-epochs, respectively (13), are not associated with any major change in CO_2 concentrations. In sharp contrast, modern rates of atmospheric C emission (~9 Pg year^{-1}) are probably the highest of the Cenozoic era (the past 65 Ma), likely surpassing even those of the Paleocene-Eocene Thermal Maximum (68).

The Antarctic ice core record shows steady enrichment in δ^{13}C values from the Late Pleistocene to the Mid-Holocene time (66, 67), reflecting carbon uptake by the terrestrial biosphere and carbon release from oceans (Fig. 5A) (66), but it shows no changes at the proposed Mid- and Late Holocene sub-epoch boundaries. The Antarctic ice record shows approximately constant CO_2 and

δ^{13}C values continuing from 1200 to 1600 CE (Fig. 5B) (69). A short-lived dip at ~1610 CE of about 10 ppm in the CO_2 curve, with a synchronous minor enrichment in δ^{13}C, has been proposed as a marker for the start of the Anthropocene (5), although these fluctuations do not exceed natural Holocene variability (Fig. 5A) (70). The most pronounced change in atmospheric CO_2 concentrations is the ~120-ppm increase since ~1850 CE (Fig. 5, B and C) (69), including a rise of ~2 ppm year^{-1} over the past 50 years. This coincides with a steep fall (>2‰) in δ^{13}C atmospheric CO_2 to ~–8.5‰ (Fig. 5C) (69), due to an increase in ^{12}C from burning fossil hydrocarbons. This isotopic signature also forms part of the permanent record, because it is inscribed in archives such as tree rings, limestones, and calcareous fossils.

Ice core records show atmospheric methane (CH_4) concentrations ranging from 590 to 760 parts per billion (ppb) through much of the Holocene (71–75), up to 1700 CE. This is followed by an unprecedented increase to 1700 ppb by 2004 CE (72), some 900 ppb higher than what has been recorded in Antarctic ice cores at any time in the past 800,000 years (76), with levels rising above Mid- to Late Pleistocene and Holocene maxima by ~1875 CE (Fig. 5D). The δ^{13}C curve for CH_4 shows a marked decrease of ~1.5‰ from ~1500 to 1700 CE, perhaps in response to reduced biomass burning (72), and a subsequent abrupt rise from ~1875 CE to the present of ~2.5‰, reflecting increasing pyrogenic emissions.

Climate change and rates of sea-level change since the end of the last ice Age

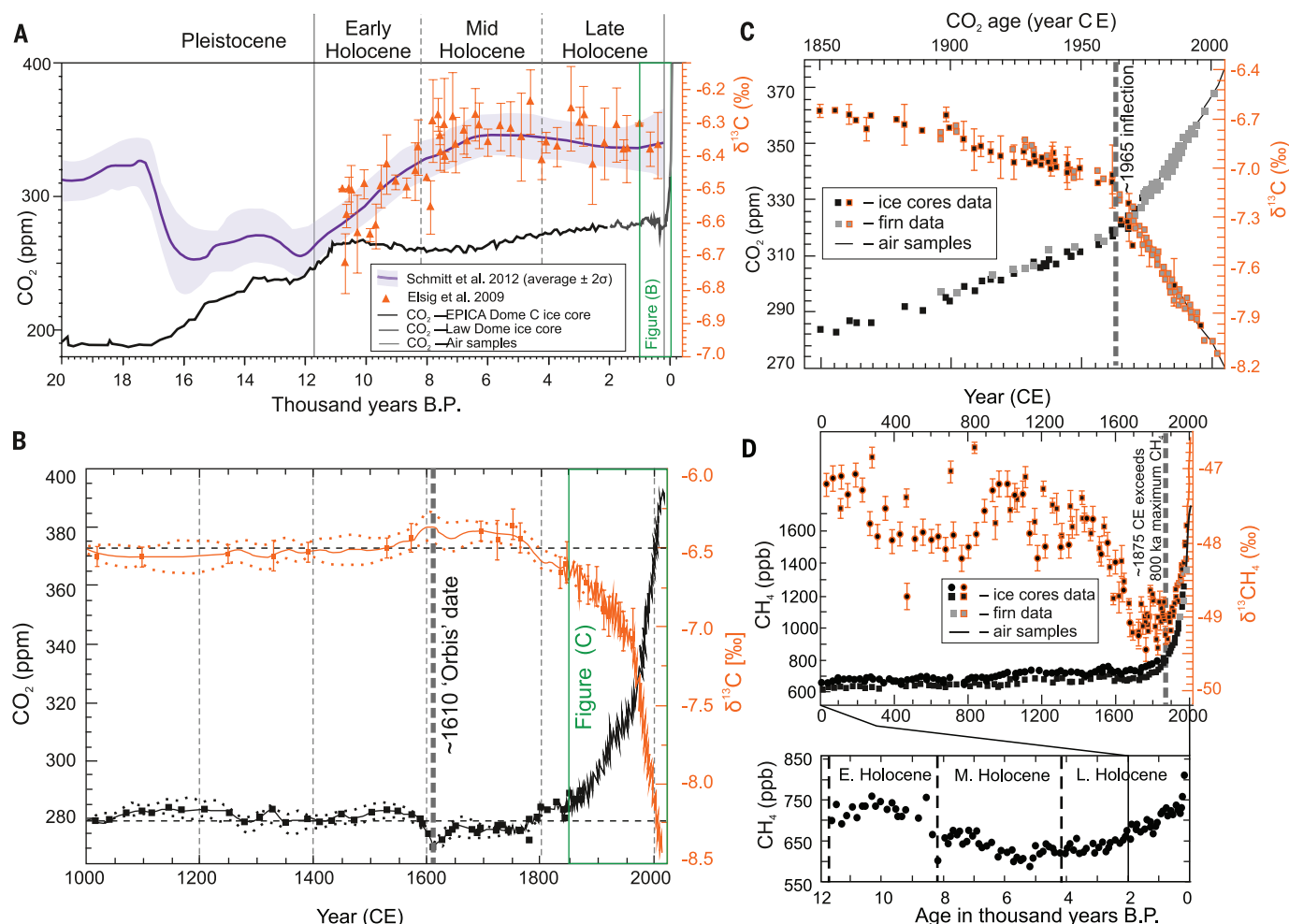The proposed subdivision of the Holocene epoch into sub-epochs is based on proxy signals for

Fig. 5. Perturbations of the carbon cycle evidenced by glaciochemical CO₂ and CH₄ concentrations and carbon isotopic ratios. (**A**) Atmospheric CO₂ from the Antarctic Law Dome and EPICA (European Project for Ice Coring in Antarctica) Dome C ice cores, with observational data [from (69) and references therein] and δ¹³C from atmospheric CO₂ (66, 67). (**B**) CO₂ concentration and δ¹³C from atmospheric CO₂ from the Law Dome ice cores (69) for the time interval indicated by the green rectangle in (A), showing a 10-ppm dip in CO₂ recognized as the Orbis event (5). (**C**) CO₂ concentration and δ¹³C from atmospheric CO₂ from the Law Dome ice core, firn data, and air samples (69) for the time period indicated by the green rectangle in (B), showing inflections at ~1965 CE. (**D**) Antarctic (squares) and Greenland (circles) ice core and firn records for CH₄ concentration and δ¹³C for atmospheric CH₄ for the past two millennia (72–75) (top), with Greenland ice core CH₄ data for the Holocene (bottom) (71).

climate change (*13*). Greenland ice cores show abrupt brief cooling events, expressed as decreases in δ¹⁸O values, at 11,400, 9300, and 8200 yr B.P. (Fig. 6A) (*77*), the lattermost of which would define the start of the proposed Middle Holocene (*13*). These events are less apparent in equivalent Antarctic ice cores (Fig. 6A) (*78*). A 4200-yr B.P. climate shift, which would mark the start of the proposed Upper Holocene (*13*), is not expressed in these curves. The overall trend during the Mid- to Late Holocene was of gradual cooling (Fig. 6B), which culminated in the Little Ice Age from 1250 to 1800 CE (Fig. 6C). The cooling followed an orbitally related insolation decline, with small fluctuations representing changes in solar intensity, which are controlled by modulators such as the 208-year Suess cycle (*79*). Given that the orbital trend is continuing, Earth should still be cooling. However, increased anthropogenic emissions of greenhouse gases have instead

caused the planet to warm abnormally fast, overriding the orbitally induced climate cycle.

The shift to climate warming (Fig. 6C) (*80*, *81*) is first indicated by a slight change toward less negative δ¹⁸O in Greenland ice starting at ~1900 CE (Fig. 6A). This shift is well outside the natural envelope of declining temperature change for the past 1400 years (Fig. 6C), mainly due to greenhouse gases released from burning of fossil fuels and deforestation (*79*, *81*, *82*). An average global temperature increase of 0.6° to 0.9°C between 1906 and 2005 CE, with a doubling of the rate of warming over the past 50 years (*83*), is beginning to exceed Holocene natural variability (Figs. 6, B and C) in the Northern Hemisphere and is already above Holocene maxima in the tropics and Southern Hemisphere. The change in δ¹⁸O since 1900 CE in Greenland ice cores (Fig. 6A) is of a smaller magnitude than that of the 8200–yr B.P. cooling event marking the base of the proposed Middle

Holocene, but it is larger than that at the base of the proposed Upper Holocene.

Average global sea levels are currently higher than at any point within the past ~115,000 years (*84*), since the termination of the last interglacial of the Pleistocene epoch. The physical expression of sea-level change in the geological record is the displacement of sedimentary facies, for which the rate of change of sea level relative to rates of sediment accumulation and subsidence due to compaction is crucial. For example, rapid sea-level rise can cause delta tops to flood, producing sharp transitions into overlying relatively deep marine and anoxic muds, marking a flooding surface. By the time of peak sea level, the rate of rise is slower, and fluvial systems can resupply sediment to re-establish deltas as progradational successions building up and out from the coast.

Very high rates of sea-level change (>40 mm year⁻¹) occurred at about 14,000 to 14,300 yr B.P.

during the Bølling warming event, associated with rapid ice sheet disintegration during the transition between the last glacial phase and the current interglacial phase (*85*). The high rate of rise caused widespread inundation of coastal areas, and sedimentary facies back-stepped (retrograded landward).

The past 7000 years of the Holocene epoch, when ice volumes stabilized near present-day values, provide the baseline for discussion of anthropogenic contributions. Relative sea-level records indicate that from ~7000 to 3000 yr B.P., global mean sea level rose ~2 to 3 m to nearly present-day levels (*84*). Based on local sea-level records spanning the past 2000 years, there is medium confidence that fluctuations in global mean sea level during this interval have not exceeded ~0.25 m on time scales of a few hundred years. As a consequence, coastlines have been more or less fixed, and sediment accumulation within beaches, tidal flats, and deltas has been progradational.

The most robust signal, captured in salt marsh records from both the Northern and Southern Hemispheres, supports a transition from relatively low rates of change during the Late Holocene (<1 mm year^{-1}) to modern rates of 3.2 ± 0.4 mm year^{-1} from 1993 to 2010 CE (*84*). By combining paleo–sea-level records with tide gauge records at the same localities, it is clear that sea level began to rise above the Late Holocene background rate between 1905 and 1945 CE (*86*); if continued, this trend will lead to a return to dominantly retrogradational shifts in sedimentary facies along coastal zones. However, reconstructions from the U.S. Atlantic coast suggest that the rate of sea-level rise is not linear (*87*). A rate of 0.06 to 0.39 mm year^{-1} during the 18th century shows a change between 1827 and 1860 CE to a late–19th century rate of 1.22 to 1.53 mm year^{-1}, and a secondary and less pronounced change from 1924 to 1943 CE to a subsequent late 20th century rate of 1.9 to 2.22 mm year^{-1} (*87*). The timing of the inflections in this rising sea-level curve matches, with a delay of about a decade, the stepped changes in CO_2 concentrations (Fig. 5C).

Compared with other stratigraphic changes described above, the climate and sea-level signals of the Anthropocene are not yet as strongly expressed, in part because they reflect the combined effects of fast and slow climate feedback mechanisms. However, given that anthropogenic forcing is driving these changes, they are likely to exceed the envelope of not only Holocene but Quaternary baseline conditions (*79*). Projections of continued warming due to greenhouse gases (*82*), even with reductions below current emissions levels, suggest that by 2070, Earth will be at its hottest since the last interglacial period ~125,000 years ago [Figure 5.3 in (*82*)]—and hence hotter than it has been for most, if not all, of the time since modern humans emerged as a species 200,000 years ago.

Changes in global average surface temperature and increases in sea level are manifestations of changes in the surface energy balance. Perhaps a more fundamental measure of human perturba-
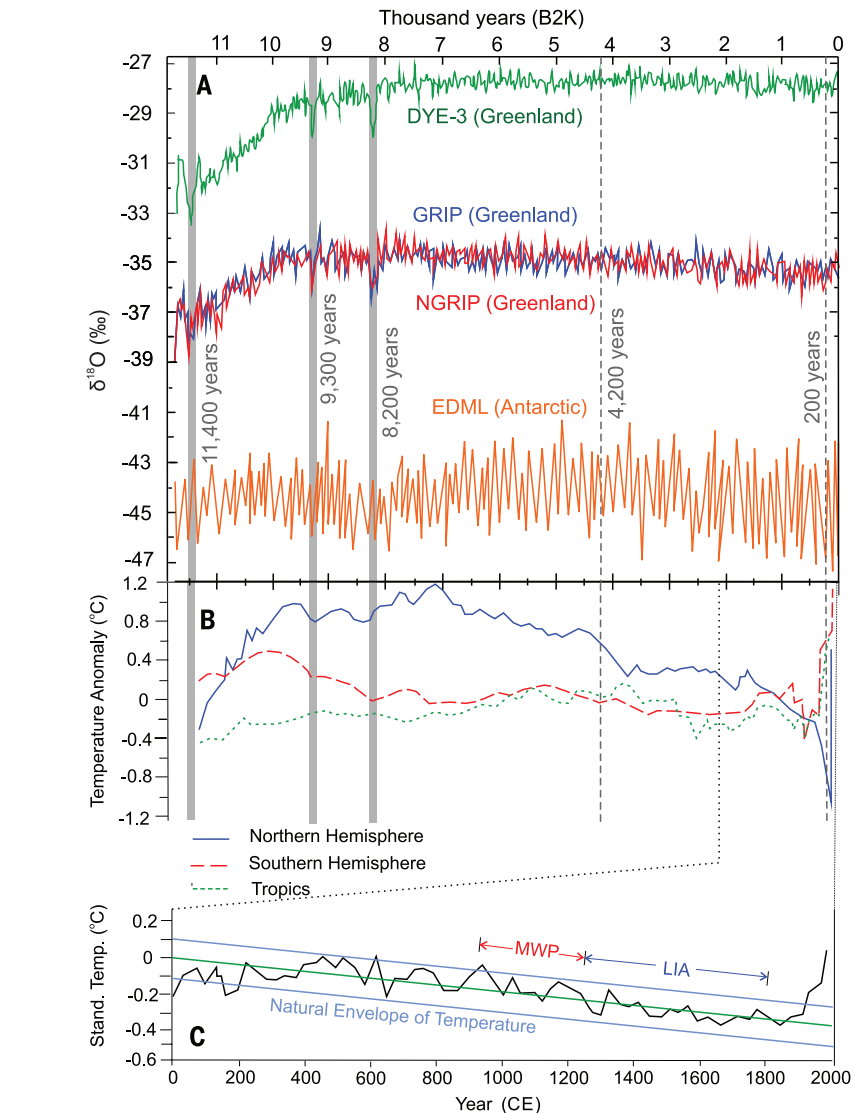

Fig. 6. Climate variations during the Holocene, indicated by oxygen isotopic ratios and modeled temperature variations. (**A**) Holocene profiles of δ^{18}O from three Greenland ice cores, with three short-duration cooling events indicated by shading (*77*), shown with an Antarctic ice core profile for comparison (EDML, EPICA Dronning Maud Land Ice Core) (*78*). (**B**) Temperature reconstructions for the Holocene and global temperatures for the past 2000 years [B2K, before 2000 CE (*81*)]. (**C**) Standardized global mean temperature for the past 2000 years, represented by 30-year means (*80, 81*), showing the natural temperature envelope for the past 2000 years [based on (*79*)]. The Little Ice Age (LIA) and the Medieval Warm Period (MWP, also known as the Medieval Climatic Anomaly) of the Northern Hemisphere are indicated.

tion of the climate system is the human-driven change to the planetary energy balance at Earth's surface, as measured by changes in radiative forcing. Human activities, primarily the burning of fossil hydrocarbons, have increased the radiative forcing by 2.29 (1.13 to 3.33) W m^{-2} relative to 1750 CE, with a more rapid increase since 1970 CE than during prior decades. Overwhelming the natural changes in radiative forcing during the Late Holocene (solar irradiance and volcanic aerosols), which are estimated to be 0.05 (0.00 to 0.10) W m^{-2} (*82*), the anthropogenic energy imbalance is poised to amplify strati-

graphic signals associated with warming and sea-level rise.

Biotic change as an indicator of the Anthropocene

Most Phanerozoic time intervals are defined using either the first or last appearance of key fossils (*29*). Evolution and extinction rates are mostly too slow and diachronous to provide an obvious biological marker for the start of the Anthropocene, but important biotic change has taken place recently (*88*). Although Earth still retains most of the species that were present at the start
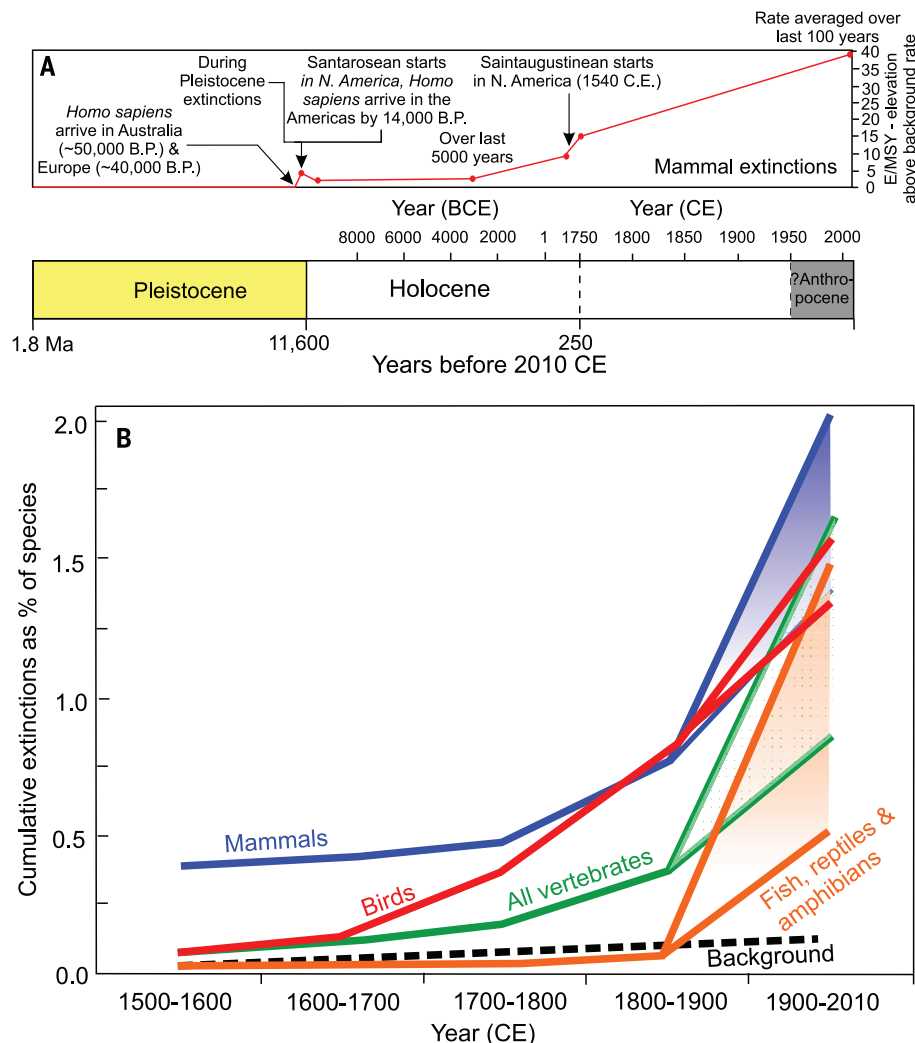
Fig. 7. Increased rates of vertebrate extinctions. (**A**) The approximate rise in mammal extinction rates calculated over varying time intervals, as extended backward from 2010 CE (Ma, millions of years ago). Lines indicate the amount by which extinction rates exceed 1.8 extinctions per million species years (E/MSY) [see (*89*); sourced from (*22*)]. (**B**) Cumulative vertebrate species extinctions as a percentage of total species, with ranges (shaded) between conservative rates (including extinctions, extinctions in the wild, and possible extinctions) and lower highly conservative rates (verified extinctions only). A background rate of 2.0 E/MSY is shown for comparison [after (*89*)].

of the Holocene, even conservative estimates of extinction rates since 1500 CE are far above mean per-million-year background rates (Fig. 7A), with a notable increase from the 19th century onward (*89*) (Fig. 7B). Current trends of habitat loss and overexploitation, if maintained, would push Earth into the sixth mass extinction event (with ~75% of species extinct) in the next few centuries (*90*), a process that is probably already underway (*89*).

Irrespective of the number of extinctions, species assemblages and relative abundances have been altered worldwide. This is especially true in recent decades because of geologically unprecedented transglobal species invasions and biological assemblage changes associated with agriculture on land and fishing in the sea (*91*). The terrestrial biosphere has undergone a dramatic modification from 1700 CE, when almost 50% of the global ice-free land area was wild and

only ~5% was intensively used by humans, to 2000 CE, when the respective percentages were 25% and 55% (*92*). The paleontological expression of these assemblages will markedly differ from the typical Holocene fossil record as recognizable, novel biostratigraphic zones (*93*), and the new assemblages of species have already permanently reconfigured Earth's biological trajectory. These biotic changes are not synchronous, but they accelerated after 1500 CE on land (*94*) and in the seas, affecting both micro- and macrobiota (*52*).

The case for a new epoch

The stratigraphic signatures described above (Fig. 1) are either entirely novel with respect to those found in the Holocene and preexisting epochs or quantitatively outside the range of variation of the proposed Holocene subdivisions. Furthermore, most proximate forcings of these

signatures are currently accelerating. These distinctive attributes of the recent geological record support the formalization of the Anthropocene as a stratigraphic entity equivalent to other formally defined geological epochs. The boundary should therefore be placed following the procedures of the International Commission on Stratigraphy.

If such formalization is to be achieved, however, further work is required. First, it needs to be determined how the Anthropocene is to be defined, whether by GSSA (calendar age), GSSP [reference point in a stratal section (*10*)], or a combination of both. Whichever is ultimately chosen, the location and comparative analyses of candidate stratotype sections are necessary, not least to explore how effectively any chosen levels may be traced and correlated within stratal archives. This is linked to the question of when exactly the Anthropocene may be determined to begin. Our analysis is more consistent with a beginning in the mid-20th century, and a number of options have already been suggested within that interval, ranging from 1945 to 1964 CE (*5*, *10*). There is also the question, which is still under debate, of whether it is helpful to formalize the Anthropocene or better to leave it as an informal, albeit solidly founded, geological time term, as the Precambrian and Tertiary currently are (*95*). This is a complex question, in part because, quite unlike other subdivisions of geological time, the implications of formalizing the Anthropocene reach well beyond the geological community. Not only would this represent the first instance of a new epoch having been witnessed firsthand by advanced human societies, it would be one stemming from the consequences of their own doing.

REFERENCES AND NOTES

1. W. Steffen, J. Grinevald, P. Crutzen, J. McNeill, The Anthropocene: Conceptual and historical perspectives. *Philos. Trans. R. Soc. London Ser. A* **369**, 842–867 (2011). doi: 10.1098/rsta.2010.0327; pmid: 21282150
2. A. Malm, A. Hornborg, The geology of mankind? A critique of the Anthropocene narrative. *Anthropocene Rev.* **1**, 62–69 (2014). doi: 10.1177/2053019613516291
3. W. F. Ruddiman, The anthropogenic greenhouse era began thousands of years ago. *Clim. Change* **61**, 261–293 (2003). doi: 10.1023/B:CLIM.0000004577.17928.fa
4. W. F. Ruddiman, The Anthropocene. *Annu. Rev. Earth Planet. Sci.* **41**, 45–68 (2013). doi: 10.1146/annurev-earth-050212-123944
5. S. L. Lewis, M. A. Maslin, Defining the Anthropocene. *Nature* **519**, 171–180 (2015). doi: 10.1038/nature14258; pmid: 25762280
6. P. J. Crutzen, Geology of mankind. *Nature* **415**, 23 (2002). doi: 10.1038/415023a; pmid: 11780095
7. J. Zalasiewicz *et al.*, Are we now living in the Anthropocene? *GSA Today* **18**, 4–8 (2008). doi: 10.1130/GSAT01802A.1
8. W. Steffen, J. Crutzen, J. R. McNeill, The Anthropocene: Are humans now overwhelming the great forces of nature? *Ambio* **36**, 614–621 (2007). doi: 10.1579/0044-7447(2007)36[614:TAAHNO]2.0.CO;2; pmid: 18240674
9. W. Steffen, W. Broadgate, L. Deutsch, O. Gaffney, C. Ludwig, The trajectory of the Anthropocene: The Great Acceleration. *Anthropocene Rev.* **2**, 81–98 (2015). doi: 10.1177/2053019614564785
10. J. Zalasiewicz *et al.*, When did the Anthropocene begin? A midtwentieth century boundary level is stratigraphically optimal. *Quat. Int.* **383**, 196–203 (2015). doi: 10.1016/j.quaint.2014.11.045
11. B. Pillans, P. Gibbard, "The Quaternary Period," in *The Geologic Time Scale*, F. M. Gradstein, J. Ogg, M. Schmitz, G. Ogg, Eds. (Elsevier B.V., 2012), pp. 979–1010.
12. J. Remane *et al.*, Guidelines for the establishment of global chronostratigraphic standards by the International Commission on Stratigraphy (ICS). *Episodes* **19**, 77–81 (1996).

13. M. J. C. Walker et al., Formal subdivision of the Holocene Series/ Epoch: A discussion paper by a Working Group of INTIMATE (Integration of ice-core, marine and terrestrial records) and the Subcommission on Quaternary Stratigraphy (International Commission on Stratigraphy). J. Quat. Sci. 27, 649–659 (2012).

14. I. McDougall, F. H. Brown, J. G. Fleagle, Stratigraphic placement and age of modern humans from Kibish, Ethiopia. Nature 433, 733–736 (2005). doi: 10.1038/nature03258; pmid: 15716951

15. "Population," History Database of the Global Environment (Netherlands Environmental Assessment Agency, Bilthoven, Netherlands, 2013); http://themasites.pbl.nl/tridion/en/ themasites/hyde/basicdrivingfactors/population/index-2.html.

16. K. Klein Goldewijk, A. Beusen, P. Janssen, Long-term dynamic modeling of global population and built-up area in a spatially explicit way: HYDE 3.1. Holocene 20, 565–573 (2010). doi: 10.1177/0959683609356587

17. A. D. Barnosky et al., Prelude to the Anthropocene: Two new North American Land Mammal Ages (NALMAs). Anthropocene Rev. 1, 225–242 (2014). doi: 10.1177/2053019614547433

18. C. N. Waters, J. A. Zalasiewicz, M. Williams, M. A. Ellis, A. M. Snelling, "A stratigraphical basis for the Anthropocene?," in A Stratigraphical Basis for the Anthropocene, C. N. Waters, J. A. Zalasiewicz, M. Williams, M. A. Ellis, A. M. Snelling, Eds. (Geological Society, London, 2014), pp. 1–21.

19. J. R. Ford, S. J. Price, A. H. Cooper, C. N. Waters, "An assessment of lithostratigraphy for anthropogenic deposits," in A Stratigraphical Basis for the Anthropocene, C. N. Waters, J. A. Zalasiewicz, M. Williams, M. A. Ellis, A. M. Snelling, Eds. (Geological Society, London, 2014), pp. 55–89.

20. J. Zalasiewicz, R. Kryza, M. Williams, "The mineral signature of the Anthropocene," in A Stratigraphical Basis for the Anthropocene, C. N. Waters, J. A. Zalasiewicz, M. Williams, M. A. Ellis, A. M. Snelling, Eds. (Geological Society, London, 2014), pp. 109–117.

21. M. Edgeworth et al., Diachronous beginnings of the Anthropocene: The lower bounding surface of anthropogenic deposits. Anthropocene Rev. 2, 33–58 (2015). doi: 10.1177/2053019614565394

22. J. Zalasiewicz, M. Williams, C. N. Waters, A. D. Barnosky, P. Haff, "Anthropocene," in Origins, O. Seberg, D. A. Harper, Eds. (Cambridge Univ. Press, in press).

23. U.S. Geological Survey, in Historical Statistics for Mineral and Material Commodities in the United States, T. D. Kelly, G. R. Matos, Eds. (U.S. Geological Survey Data Series 140, U.S. Geological Survey, 2010); http://minerals.usgs.gov/ minerals/pubs/historical-statistics/cement-use.pdf.

24. Plastics – the Facts 2013. An Analysis of European Latest Plastics Production, Demand and Waste Data (PlasticsEurope, 2013); www.plasticseurope.org/documents/document/ 20131014095824-final_plastics_the_facts_2013_published_ october2013.pdf.

25. P. L. Corcoran, Benthic plastic debris in marine and fresh water environments. Environ. Sci. Processes Impacts 17, 1363–1369 (2015). doi: 10.1039/C5EM00188A; pmid: 26129903

26. R. C. Thompson et al., Lost at sea: Where is all the plastic? Science 304, 838 (2004). doi: 10.1126/science.1094559; pmid: 15131299

27. J. R. Jambeck et al., Plastic waste inputs from land into the ocean. Science 347, 768–771 (2015). doi: 10.1126/science.1260352; pmid: 25678662

28. J. Zalasiewicz, M. Williams, C. N. Waters, A. D. Barnosky, P. Haff, The technofossil record of humans. Anthropocene Rev. 1, 34–43 (2014). doi: 10.1177/2053019613514953

29. A. G. Smith, T. Barry, P. Bown, J. Cope, A. Gale, P. L. Gibbard, J. Gregory, M. Hounslow, D. Kemp, R. Knox, J. Marshall, M. Oates, P. Rawson, J. Powell, C. Waters, "GSSPs, global stratigraphy and correlation," in Strata and Time: Probing the Gaps in Our Understanding, D. G. Smith, R. J. Bailey, P. M. Burgess, A. J. Fraser, Eds. (Special Publication 404, Geological Society, London, 2014), pp. 37–67.

30. T. Novakov et al., Large historical changes of fossil-fuel black carbon aerosols. Geophys. Res. Lett. 30, 1324 (2003). doi: 10.1029/2002GL016345

31. F. Oldfield, Can the magnetic signatures from inorganic fly ash be used to mark the onset of the Anthropocene? Anthropocene Rev. 2, 3–13 (2015). doi: 10.1177/2053019614534402

32. N. L. Rose, Spheroidal carbonaceous fly ash particles provide a globally synchronous stratigraphic marker for the Anthropocene. Environ. Sci. Technol. 49, 4155–4162 (2015). doi: 10.1021/acs.est.5b00543; pmid: 25790111

33. G. T. Swindles et al., Spheroidal carbonaceous particles are a defining stratigraphic marker for the Anthropocene. Sci. Rep. 5, 10264 (2015). doi: 10.1038/srep10264; pmid: 26020614

34. M. C. Harvey, S. C. Brassell, C. M. Belcher, A. Montanari, Combustion of fossil organic matter at the Cretaceous-Paleogene (K-P) boundary. Geology 36, 355–358 (2008). doi: 10.1130/G24646A.1

35. R. LeB. Hooke, J. F. Martín-Duque, Land transformation by humans: A review. GSA Today 22, 4–10 (2012).

36. J. Zalasiewicz, M. Williams, C. N. Waters "Can an Anthropocene Series be defined and recognized?," in A Stratigraphical Basis for the Anthropocene, C. N. Waters, J. A. Zalasiewicz, M. Williams, M. A. Ellis, A. M. Snelling, Eds. (Geological Society, London, 2014), pp. 39–53.

37. J. Zalasiewicz, C. N. Waters, M. Williams, Human bioturbation, and the subterranean landscape of the Anthropocene. Anthropocene 6, 3–9 (2014). doi: 10.1016/j.ancene.2014.07.002

38. I. Douglas, N. Lawson, The human dimensions of geomorphological work in Britain. J. Ind. Ecol. 4, 9–33 (2000). doi: 10.1162/108819800569771

39. E. C. Ellis, Anthropogenic transformation of the terrestrial biosphere. Philos. Trans. R. Soc. London Ser. A 369, 1010–1035 (2011). doi: 10.1098/rsta.2010.0331; pmid: 21282158

40. A. Brown, P. Toms, C. Carey, E. Rhodes, Geomorphology of the Anthropocene: Time-transgressive discontinuities of human-induced alluviation. Anthropocene 1, 3–13 (2013). doi: 10.1016/j.ancene.2013.06.002

41. P. Meyfroidt, E. F. Lambin, Global forest transition: Prospects for an end to deforestation. Annu. Rev. Environ. Resour. 36, 343–371 (2011). doi: 10.1146/annurev-environ-090710-143732

42. R. C. Sidle, A. D. Ziegler, The dilemma of mountain roads. Nat. Geosci. 5, 437–438 (2012). doi: 10.1038/ngeo1512

43. J. P. M. Syvitski, A. Kettner, Sediment flux and the Anthropocene. Philos. Trans. R. Soc. London Ser. A 369, 957–975 (2011). doi: 10.1098/rsta.2010.0329; pmid: 21282156

44. C. K. Paull, W. Ussler III, P. J. Mitts, D. W. Caress, G. J. West, Discordant ¹⁴C-stratigraphies in upper Monterey Canyon: A signal of anthropogenic disturbance. Mar. Geol. 233, 21–36 (2006). doi: 10.1016/j.margeo.2006.07.008

45. C. H. Vane et al., Chemical signatures of the Anthropocene in the Clyde estuary, UK: Sediment-hosted Pb, $^{207/206}$Pb, total petroleum hydrocarbon, polyaromatic hydrocarbon and polychlorinated biphenyl pollution records. Philos. Trans. R. Soc. London Ser. A 369, 1085–1111 (2011). doi: 10.1098/rsta.2010.0298; pmid: 21282161

46. D. C. G. Muir, N. L. Rose, "Persistent organic pollutants in the sediments of Lochnagar," in Lochnagar: The Natural History of a Mountain Lake, N. L. Rose, Ed. (Springer, Dordrecht, Germany, 2007), pp. 375–402.

47. J. R. Dean, M. J. Leng, A. W. Mackay, Is there an isotopic signature of the Anthropocene? Anthropocene Rev. 1, 276–287 (2014). doi: 10.1177/2053019614541631

48. D. E. Canfield, A. N. Glazer, P. G. Falkowski, The evolution and future of Earth's nitrogen cycle. Science 330, 192–196 (2010). doi: 10.1126/science.1186120; pmid: 20929768

49. S. R. Carpenter, E. M. Bennett, Reconsideration of the planetary boundary for phosphorus. Environ. Res. Lett. 6, 014009 (2011). doi: 10.1088/1748-9326/6/1/014009

50. J. N. Galloway et al., Transformation of the nitrogen cycle: Recent trends, questions, and potential solutions. Science 320, 889–892 (2008). doi: 10.1126/science.1136674; pmid: 18487183

51. E. A. Holland, J. Lee-Taylor, C. Nevison, J. Sulzman, Global N Cycle: Fluxes and N₂O Mixing Ratios Originating from Human Activity. Data Set (Oak Ridge National Laboratory Distributed Active Archive Center, Oak Ridge, TN, 2005); http://daac.ornl. gov/cgi-bin/dsviewer.pl?ds_id=797.

52. I. P. Wilkinson, C. Poirier, M. J. Head, C. D. Sayer, J. Tibby, "Microbiotic signatures of the Anthropocene in marginal marine and freshwater palaeoenvironments," in A Stratigraphean Basis for the Anthropocene, C. N. Waters, J. A. Zalasiewicz, M. Williams, M. A. Ellis, A. M. Snelling, Eds. (Geological Society, London, 2014), pp. 185–219.

53. G. W. Holtgrieve et al., A coherent signature of anthropogenic nitrogen deposition to remote watersheds of the Northern Hemisphere. Science 334, 1545–1548 (2011). doi: 10.1126/ science.1212267; pmid: 22174250

54. A. P. Wolfe et al., Stratigraphic expressions of the Holocene–Anthropocene transition revealed in sediments from remote lakes. Earth Sci. Rev. 116, 17–34 (2013). doi: 10.1016/j.earscirev.2012.11.001

55. M. G. Hastings, D. M. Sigman, E. J. Steig, Glacial/interglacial changes in the isotopes of nitrate from the Greenland Ice Sheet Project 2 (GISP2) ice core. Global Biogeochem. Cycles 19, GB4024 (2005). doi: 10.1029/2005GB002502

56. M. G. Hastings, J. C. Jarvis, E. J. Steig, Anthropogenic impacts on nitrogen isotopes of ice-core nitrate. Science 324, 1288 (2009). doi: 10.1126/science.1170510; pmid: 19498161

57. E. W. Wolff, "Ice sheets and the Anthropocene," in A Stratigraphical Basis for the Anthropocene, C. N. Waters, J. A. Zalasiewicz, M. Williams, M. A. Ellis, A. M. Snelling, Eds. (Geological Society, London, 2014), pp. 255–263.

58. A. Gałuszka, Z. M. Migaszewski, J. Zalasiewicz, "Assessing the Anthropocene with geochemical methods," in A Stratigraphical Basis for the Anthropocene, C. N. Waters, J. A. Zalasiewicz, M. Williams, M. A. Ellis, A. M. Snelling, Eds. (Geological Society, London, 2014), pp. 221–238.

59. K. E. Jarvis, S. J. Parry, J. M. Piper, Temporal and spatial studies of autocatalyst-derived platinum, rhodium, and palladium and selected vehicle-derived trace elements in the environment. Environ. Sci. Technol. 35, 1031–1036 (2001). doi: 10.1021/es0001512; pmid: 11347910

60. UNSCEAR-United Nations Scientific Committee on the Effects of Atomic Radiation, Sources and Effects of Ionizing Radiation (United Nations, New York, 2000).

61. C. N. Waters et al., Can nuclear weapons fallout mark the beginning of the Anthropocene Epoch? Bull. Atom. Sci. 71, 46–57 (2015). doi: 10.1177/0096340215581357

62. P. J. Reimer et al., IntCal13 and Marine13 radiocarbon age calibration curves 0–50,000 years cal BP. Radiocarbon 55, 1869–1887 (2013). doi: 10.2458/azu_js_rc.55.16947

63. Q. Hua, M. Barbetti, A. Z. Rakowski, Atmospheric radiocarbon for the period 1950–2010. Radiocarbon 55, 2059–2072 (2013). doi: 10.2458/azu_js_rc.v55i2.16177

64. G. J. Hancock, S. G. Tims, L. K. Fifield, I. T. Webster, "The release and persistence of radioactive anthropogenic nuclides," in A Stratigraphical Basis for the Anthropocene, C. N. Waters, J. A. Zalasiewicz, M. Williams, M. A. Ellis, A. M. Snelling, Eds. (Geological Society, London, 2014), pp. 265–281.

65. E. W. Wolff, Greenhouse gases in the Earth system: A palaeoclimate perspective. Philos. Trans. R. Soc. London Ser. A 369, 2133–2147 (2011). doi: 10.1098/rsta.2010.0225; pmid: 21502180

66. J. Elsig et al., Stable isotope constraints on Holocene carbon cycle changes from an Antarctic ice core. Nature 461, 507–510 (2009). doi: 10.1038/nature08393; pmid: 19779448

67. J. Schmitt et al., Carbon isotope constraints on the deglacial CO₂ rise from ice cores. Science 336, 711–714 (2012). doi: 10.1126/science.1217161; pmid: 22461496

68. Y. Cui et al., Slow release of fossil carbon during the Palaeocene–Eocene Thermal Maximum. Nat. Geosci. 4, 481–485 (2011). doi: 10.1038/ngeo1179

69. M. Rubino et al., A revised 1000 year atmospheric δ¹³C-CO₂ record from Law Dome and South Pole, Antarctica. J. Geophys. Res. 118, 8482–8499 (2013).

70. J. Zalasiewicz et al., Colonization of the Americas, 'Little Ice Age' climate, and bomb-produced carbon: Their role in defining the Anthropocene. Anthropocene Rev. 2, 117–127 (2015). doi: 10.1177/2053019615587056

71. T. Blunier, J. Chappellaz, J. Schwander, B. Stauffer, D. Raynaud, Variations in atmospheric methane concentration during the Holocene epoch. Nature 374, 46–49 (1995). doi: 10.1038/ 374046a0

72. D. F. Ferretti et al., Unexpected changes to the global methane budget over the past 2000 years. Science 309, 1714–1717 (2005). doi: 10.1126/science.1115193; pmid: 16151008

73. C. MacFarling Meure et al., Law Dome CO₂, CH₄ and N₂O ice core records extended to 2000 years BP. Geophys. Res. Lett. 33, L14810 (2006). doi: 10.1029/2006GL026152

74. C. J. Sapart et al., Natural and anthropogenic variations in methane sources during the past two millennia. Nature 490, 85–88 (2012). doi: 10.1038/nature11461; pmid: 23038470

75. L. Mitchell, E. Brook, J. E. Lee, C. Buizert, T. Sowers, Constraints on the late Holocene anthropogenic contribution to the atmospheric methane budget. Science 342, 964–966 (2013). doi: 10.1126/science.1238920; pmid: 24264988

76. L. Loulergue et al., EPICA Dome C Ice Core, 800 KYyr Methane Data. IGBP PAGES, World Data Center for Paleoclimatology, Data Contribution Series #2008-054 (National Oceanic and Atmospheric Administration/National Climatic Data Center Paleoclimatology Program, Boulder, CO, 2008); http://cdiac. ornl.gov/trends/atm_meth/ice_core_methane.html.

77. B. M. Vinther et al., A synchronized dating of three Greenland ice cores throughout the Holocene. J. Geophys. Res. 111, D13102 (2006). doi: 10.1029/2005JD006921

78. T. Felis et al., Pronounced interannual variability in tropical South Pacific temperatures during Heinrich Stadial 1. Nat. Commun. 3, 965 (2012). doi: 10.1038/ncomms1901; pmid: 22828625

79. C. P. Summerhayes, Earth's Climate Evolution (Wiley-Blackwell, 2015).

80. M. Ahmed *et al.*, Continental-scale temperature variability during the past two millennia. *Nat. Geosci.* **6**, 339–346 (2013). doi: 10.1038/ngeo1797

81. H. Wanner, L. Mercolli, M. Grosjean, S. P. Ritz, Holocene climate variability and change; a data-based review. *J. Geol. Soc. London* **172**, 254–263 (2015). doi: 10.1144/jgs2013-101

82. IPCC, *Climate Change 2013: The Physical Science Basis. Contribution of Working Group I to the Fifth Assessment Report of the Intergovernmental Panel on Climate Change*, T. F. Stocker *et al.*, Eds. (Cambridge Univ. Press, 2013).

83. J. R. Hansen, R. Ruedy, M. Sato, K. Lo, Global surface temperature change. *Rev. Geophys.* **48**, RG4004 (2010). doi: 10.1029/2010RG000345

84. J. A. Church, P. U. Clark, A. Cazenave, J. M. Gregory, S. Jevrejeva, A. Levermann, M. A. Merrifield, G. A. Milne, R. S. Nerem, P. D. Nunn, A. J. Payne, W. T. Pfeffer, D. Stammer, A. S. Unnikrishnan, "Sea level change," in *Climate Change 2013: The Physical Science Basis. Contribution of Working Group I to the Fifth Assessment Report of the Intergovernmental Panel on Climate Change*, T. F. Stocker *et al.*, Eds. (Cambridge Univ. Press, 2013), pp. 1137–1216.

85. P. Deschamps *et al.*, Ice-sheet collapse and sea-level rise at the Bølling warming 14,600 years ago. *Nature* **483**, 559–564 (2012). doi: 10.1038/nature10902; pmid: 22460900

86. R. Gehrels, P. L. Woodworth, When did modern rates of sea-level rise start? *Global Planet. Change* **100**, 263–277 (2013). doi: 10.1016/j.gloplacha.2012.10.020

87. A. C. Kemp *et al.*, Relative sea-level change in Connecticut (USA) during the last 2200 yrs. *Earth Planet. Sci. Lett.* **428**, 217–229 (2015). doi: 10.1016/j.epsl.2015.07.034

88. A. D. Barnosky, "Palaeontological evidence for defining the Anthropocene," in *A Stratigraphical Basis for the Anthropocene*, C. N. Waters, J. A. Zalasiewicz, M. Williams, M. A. Ellis, A. M. Snelling, Eds. (Geological Society, London, 2014), pp. 149–165.

89. G. Ceballos *et al.*, Accelerated modern human-induced species losses: Entering the sixth mass extinction. *Sci. Adv.* **1**, e1400253 (2015). doi: 10.1126/sciadv.1400253; pmid: 26601195

90. A. D. Barnosky, N. Matzke, S. Tomiya, G. O. U. Wogan, B. Swartz, T. B. Quental, C. Marshall, J. L. McGuire, E. L. Lindsey, K. C. Maguire, B. Mersey, E. A. Ferrer, Has the Earth's sixth mass extinction already arrived? *Nature* **471**, 51–57 (2011). doi: 10.1038/nature09678

91. M. Williams *et al.*, The Anthropocene biosphere. *Anthropocene Rev.* **2**, 196–219 (2015). doi: 10.1177/2053019615591020

92. E. C. Ellis, K. K. Goldewijk, S. Siebert, D. Lightman, N. Ramankutty, Anthropogenic transformation of the biomes, 1700 to 2000. *Glob. Ecol. Biogeogr.* **19**, 589–606 (2010).

93. S. M. Kidwell, Biology in the Anthropocene: Challenges and insights from young fossil records. *Proc. Natl. Acad. Sci. U.S.A.* **112**, 4922–4929 (2015). doi: 10.1073/pnas.1403660112; pmid: 25901315

94. J. R. McNeill, "Biological exchanges in world history," in *The Oxford Handbook of World History*, J. Bentley, Ed. (Oxford Univ. Press, 2011), pp. 325–342.

95. W. F. Ruddiman, E. C. Ellis, J. O. Kaplan, D. Q. Fuller, Defining the epoch we live in. *Science* **348**, 38–39 (2015). doi: 10.1126/science.aaa7297; pmid: 25838365